

Beyond Tree Level with Solar Neutrinos: Towards Measuring the Flavor Composition and CP Violation

Vedran Brdar^{1,*} and Xun-Jie Xu^{2,†}

¹*Theoretical Physics Department, CERN, 1 Esplanade des Particules, 1211 Geneva 23, Switzerland*

²*Institute of High Energy Physics, Chinese Academy of Sciences, Beijing 100049, China*

After being produced as electron neutrinos (ν_e), solar neutrinos partially change their flavor to ν_μ and ν_τ en route to Earth. Although the flavor ratio of the ν_e flux to the total flux has been well measured, the $\nu_\mu : \nu_\tau$ composition has not yet been experimentally probed. In this work we investigate the potential of the next-generation experiments for measuring the $\nu_\mu : \nu_\tau$ flavor ratio by utilizing flavor-dependent radiative corrections in the cross sections for ν_μ and ν_τ scattering. Since the transition probabilities of ν_e to ν_μ and ν_τ depend on the leptonic CP phase, we also investigate the sensitivity to the CP phase and show that a statistical significance of $\sim 1\sigma$ could be reached through precision measurements of solar neutrino spectra.

Introduction. The first observation of solar neutrinos at the Homestake experiment [1] was not consistent with the theoretical predictions from Bahcall [2] and this turned out to be the first experimental hint for neutrino oscillation [3–7]. This phenomenon implies that neutrinos produced in the Sun change flavor en route to Earth, which has by now been confirmed with a number of experiments including SNO [8, 9], Super-Kamiokande [10, 11], and Borexino [12, 13]. For recent reviews on solar neutrino physics, see [14, 15].

The modern-day solar neutrino observations have established that only about a third of neutrinos produced in the Sun arrive to Earth as electron neutrinos (ν_e), while the remaining fraction is composed of muon (ν_μ) and tau neutrinos (ν_τ). The ratio between ν_μ and ν_τ fluxes is theoretically known but it has never been measured. A full measurement of the flavor composition ($\nu_e : \nu_\mu : \nu_\tau$) would be valuable, as it would not only allow us to gain a better understanding of our nearest star, but would also make it possible to probe the transition probabilities $P_{\nu_e \rightarrow \nu_\mu}$ and $P_{\nu_e \rightarrow \nu_\tau}$ which depend on the level of the CP violation in the lepton sector (parameterized by the phase δ_{CP}). Given such dependence, solar neutrinos could serve as a complementary probe of CP violation to the near-future acceleration-based neutrino program led by DUNE [16] and Hyper-Kamiokande (HK) [17].

In this letter we propose a viable method to differentiate between solar ν_μ and ν_τ . Since solar neutrino energies do not exceed ~ 20 MeV, ν_μ and ν_τ can only be detected via elastic scattering and, at the leading order, cross sections for this process are identical for both ν_μ and ν_τ . At the next-to-leading order (NLO), however, differences arise from flavor-dependent radiative corrections [18–20]; see e.g. Fig. 1.

In this work we will be focused on solar neutrinos and the phenomenological consequences that radiative corrections in the cross section for neutrino-electron elastic scattering (eES) [21, 22] can induce. One of the advantages for considering $\nu_{\mu,\tau} + e^- \rightarrow \nu_{\mu,\tau} + e^-$ is the rather small theoretical uncertainty in the cross section which

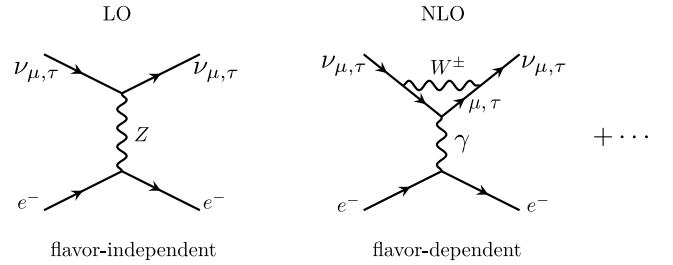


Figure 1. Feynman diagrams for $\nu_{\mu,\tau}$ scattering on electrons. The diagram on the left shows the leading order contribution whereas the one on the right illustrates the flavor-dependent NLO contribution.

is at sub-percent level [23, 24]. With sufficiently high statistics, the difference between ν_μ and ν_τ cross sections could manifest itself in the data, namely in the total number of eES events. We investigate that by considering large next-generation neutrino detectors such as HK [17], DUNE [16], JUNO [25] and THEIA [26].

Radiative corrections for eES cross section. As already introduced, in this work we will mainly consider eES, the experimental signature of which is the detection of electron recoil kinetic energy, denoted as T . The differential cross section without the inclusion of any radiative corrections reads [22]

$$\frac{d\sigma}{dT} = \frac{2G_F^2 m_e}{\pi} \left[\left(s_W^2 \pm \frac{1}{2} \right)^2 + s_W^4 \left(1 - \frac{T}{E_\nu} \right)^2 - \left(s_W^2 \pm \frac{1}{2} \right) s_W^2 \frac{m_e T}{E_\nu^2} \right], \quad (1)$$

where the + (−) sign applies for ν_e (ν_μ or ν_τ) scattering on electron. In Eq. (1), G_F is the Fermi constant, s_W stands for the sine of the weak mixing angle and m_e is the electron mass.

The difference between ν_μ and ν_τ scattering cross sections comes about at NLO [21, 22, 27]. We are in particular interested in flavor-dependent corrections,

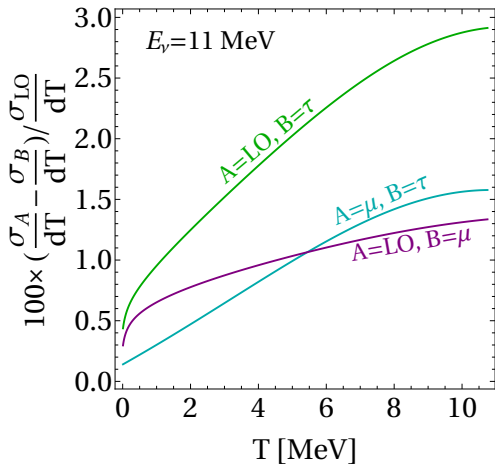


Figure 2. Comparison between the differential cross sections, normalized to the leading order one (see Eq. (1)). In particular, we would like to draw reader’s attention to the cyan line that demonstrates $\mathcal{O}(1\%)$ difference between ν_μ and ν_τ scattering cross sections. This is the effect our phenomenological study is based on.

which arise from higher-order diagrams involving μ and τ leptons in the loops, such as the right diagram in Fig. 1. This effect can be accounted for via redefinition $s_W^2 \rightarrow s_W^2(1 - \Delta)$ [19, 27] in Eq. (1); here Δ accounts for a subset of 1-loop corrections for eES and we are mostly interested in the flavor-dependent contribution $\Delta_l \equiv \alpha(6\pi s_W^2)^{-1} \text{Log}(m_W^2/m_l^2)$ where m_W and m_l are W boson and charged lepton masses, respectively. Δ_l is evaluated assuming a vanishing momentum transfer which is a reasonable approximation given the magnitude of the considered E_ν . It turns out that $\Delta_\mu - \Delta_\tau \approx 0.01$, and this propagates to $\mathcal{O}(1\%)$ difference in the cross section; the ν_μ cross section is larger than the ν_τ one, see the cyan line in Fig. 2. In the figure, we also compare each of these cross sections at 1-loop level with the respective tree-level expression (see Eq. (1)); these $\mathcal{O}(\alpha)$ effects are shown by purple and green lines, respectively. Let us stress that in making Fig. 2 as well as for our analysis presented in the next sections, we utilize results from [23, 24]. There, both electroweak and QED corrections as well as the emission of soft photons is taken into account for eES. Note that, as a cross check, we also explicitly implemented the expressions from [21] and found consistent results; for instance, the difference between ν_μ and ν_τ cross sections was found, for any value of T , to deviate from cyan line in Fig. 2 by no more than 0.1%.

The above discussion on the cross sections is important for the detection of neutrinos. However, one may also wonder about the impact of radiative corrections in neutrino propagation; after all, for the computation of the Mikheyev-Smirnov-Wolfenstein (MSW) matter potential [5–7] the same diagrams as those presented in Fig. 1 should be evaluated at a zero momentum trans-

fer. The flavor-dependent NLO effects in the propagation were studied in [28] where it was found that when summing the relevant contributions, including diagrams with neutrino scattering on both electrons and quarks (nucleons), there is a cancellation at $\mathcal{O}(\alpha)$ level for neutrinos traveling through a neutral unpolarized medium. In turn, the flavor-dependent effects in neutrino propagation arise only at $\mathcal{O}(\alpha(m_l^2/m_W^2)\text{Log}(m_W^2/m_l^2)) \approx 10^{-6}$ which is rather small. This led the authors of [29] to conclude that such smallness of flavor-dependent terms leads to virtually no sensitivity to δ_{CP} when studying solar neutrinos. In this paper we will oppose such a claim and demonstrate the sensitivity to CP violation by utilizing $\mathcal{O}(\alpha)$ differences in eES for different neutrino flavors.

Measuring the Flavor Composition. Now, let us utilize the flavor-dependent cross sections to scrutinize the potential for measuring the solar neutrino flavor composition ($\phi_{\nu_e} : \phi_{\nu_\mu} : \phi_{\nu_\tau}$) where ϕ_{ν_α} denotes the flux of ν_α . For convenience, we define

$$R_\alpha \equiv \frac{\phi_{\nu_\alpha}}{\phi_{\text{total}}}, \quad \phi_{\text{total}} \equiv \phi_{\nu_e} + \phi_{\nu_\mu} + \phi_{\nu_\tau}. \quad (2)$$

Since $R_e + R_\mu + R_\tau = 1$, only two of the ratios are independent. We also define $\bar{R}_\mu \equiv \phi_{\nu_\mu}/(\phi_{\nu_\mu} + \phi_{\nu_\tau})$ which can freely vary between 0 to 1. Here, we should stress that the flavor ratios are actually energy-dependent according to the standard MSW solution. Nevertheless, in this section, for demonstration purposes, we take them as energy-independent in the fit and investigate how well the solar neutrino flux components can be measured. This contrasts to the following section in which we study δ_{CP} sensitivity in the framework of the standard MSW solution.

To date, only R_e has been successfully measured, via combination of eES, neutrino-nucleus charged current (CC) and neutral current (NC) scattering. Among the three channels, eES and neutrino-nucleus CC scattering have different cross sections for ν_e and ν_x ($x = \mu$ or τ) while neutrino-nucleus NC scattering is flavor independent at the leading order. When combining the three channels, R_e is actually overconstrained¹ but the flavor composition $\phi_{\nu_\mu} : \phi_{\nu_\tau}$ still cannot be resolved. To measure this flavor composition, one has to include the aforementioned radiative corrections which induce small differences between ν_μ and ν_τ cross sections.

With the NLO corrections included and by taking (R_e, \bar{R}_μ) as free parameters, we perform a χ^2 -fit analysis to evaluate the potential of next-generation neutrino experiments to measure $\phi_{\nu_e} : \phi_{\nu_\mu} : \phi_{\nu_\tau}$.

The next-generation neutrino detectors will feature complementary advantages. The HK detector, which will

¹ The data from the three channels turns out to be compatible with each other; see e.g., Fig. 29 of Ref. [30].

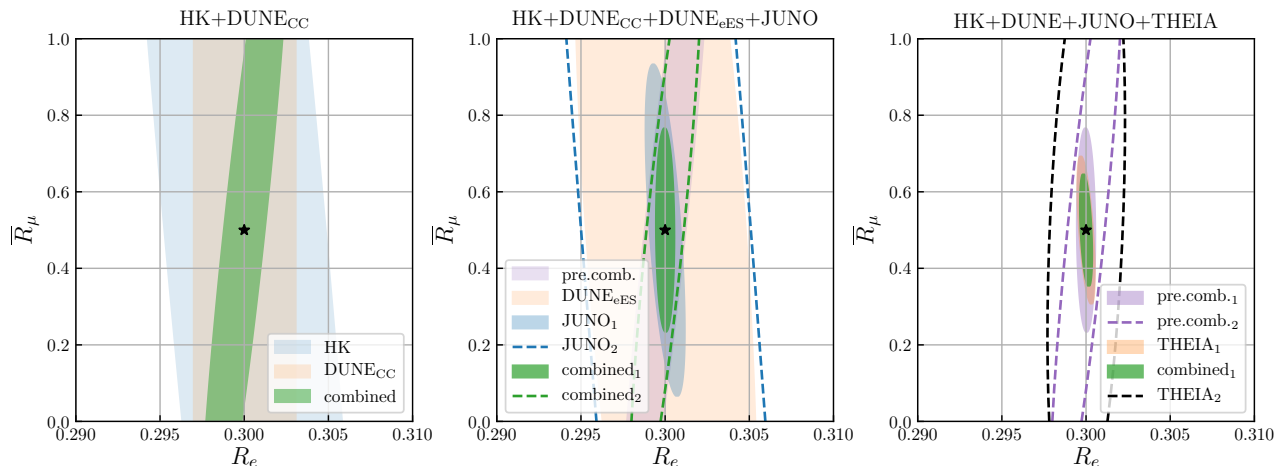


Figure 3. The capability of next-generation neutrino detectors for measuring solar neutrino flavor compositions. The subscripts 1, 2 indicate that JUNO_{1,2} and/or THEIA_{1,2} is included in the analysis—see text for details. All contours are at 1 σ CL and the assumed true value is marked by \star .

be a 187 kt water Cherenkov detector, will have the highest statistics in the eES channel at energies above a certain threshold. We assume that the threshold is the same as for Super-Kamiokande, namely $T \gtrsim 3.49$ MeV [31]. The far detector of JUNO will be a 20 kt liquid scintillator (LS) detector and will also have high statistics in the eES channel. Despite the smaller fiducial mass, its detection threshold, if neglecting cosmogenic backgrounds, could be much lower than the one at HK due to the high light yield in LS. If one only counts the yield of photoelectrons, the threshold is likely to reach $T \gtrsim 0.1$ MeV². However, cosmogenic backgrounds [33] pose the main challenge to the detection of low-energy events. In Borexino, these backgrounds are effectively reduced via a few sophisticated methods (e.g. TFC) [34], which enable Borexino to successfully detect the low-energy part (pp, ⁷Be, CNO) of solar neutrino spectrum. Since the underground depth of JUNO is about half the depth of Borexino, we anticipate that JUNO might be able to apply the same background reduction techniques to some extent. Hence, for JUNO, we consider two cases, denoted by JUNO₁ and JUNO₂. JUNO₁ simply assumes the effective reduction of cosmogenic backgrounds while JUNO₂ conservatively assumes that all eES events below 2 MeV are not discernible from the background, leading to a relatively high threshold $T \gtrsim 2$ MeV. The far detector of the DUNE experiment will contain 40 kt of liquid Ar and it is anticipated to measure solar neutrinos in both CC ($\nu_e + {}^{40}\text{Ar} \rightarrow e^- + {}^{40}\text{K}$, denoted by ArCC)

and eES channels [35]. We assume that the threshold of ArCC process at DUNE will be $E_\nu \gtrsim 7$ MeV. Very recently, the THEIA experiment has been proposed [26], with a 100 kt water-based liquid scintillator (WbLS) detector placed deep underground. A high (low) percentage of LS in WbLS would decrease (increase) its capability of measuring the direction of interacting neutrinos, but it would lead to a lower (higher) energy threshold. If pure LS is employed, it would be very similar to Borexino, which according to Refs. [36, 37] has detected pp neutrinos successfully with the threshold around 150-200 keV. If 5% WbLS is used, then it is likely that the threshold may reach 0.6 MeV [26]. As the percentage of LS is not determined yet, we consider two configurations for THEIA, namely THEIA₁ using pure LS with a 0.1 MeV threshold, and THEIA₂ using 5% WbLS with a 0.6 MeV threshold. Dark matter detectors could contribute in the NC channel by collecting coherent elastic neutrino-nucleus scattering (CE ν NS) events induced by solar neutrinos. However, the statistics of such NC events in ton-scale detectors is low (in particular, they have not been measured to date), compared to the achieved SNO (kt-scale) observations of $\nu + {}^2\text{H} \rightarrow \nu + n + p$ which is also a NC channel. The contribution of dark matter detectors for distinguishing between solar fluxes of ϕ_μ and ϕ_τ is therefore expected not to be competitive to the above introduced experiments and channels. In our analysis, the eES channel at HK, DUNE, JUNO and THEIA is studied and combined with the ArCC channel at DUNE.

² This is a reasonable assumption, given that KamLAND reached about 0.2 MeV according to Ref. [32] and JUNO will have a significantly higher yield of photoelectrons with respect to KamLAND.

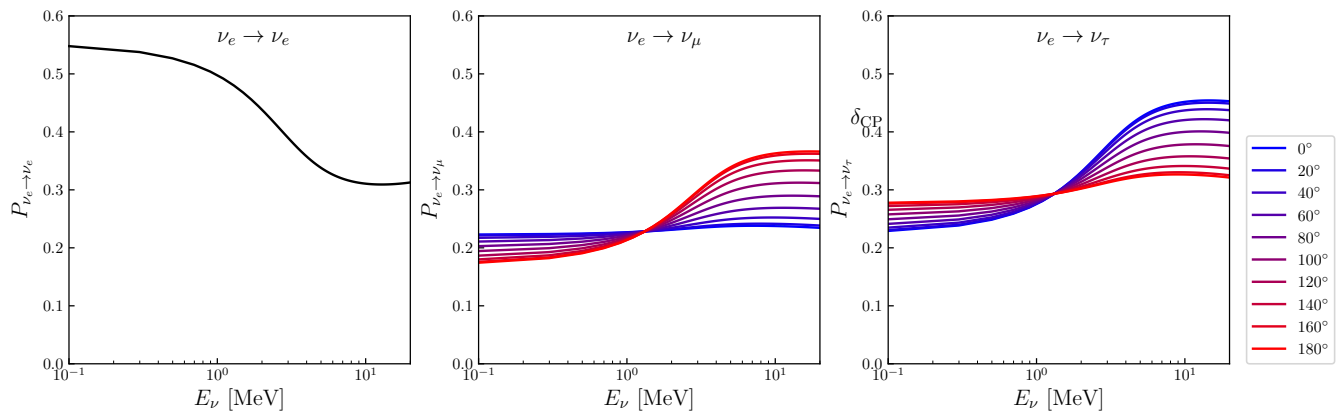


Figure 4. The solar neutrino transition probabilities $P_{\nu_e \rightarrow \nu_\alpha}(E_\nu)$ for various values of δ_{CP} .

The eES event rate reads³

$$\frac{dN}{dT} = N_e \Delta t \sum_{\alpha} \int \frac{d\sigma_{\nu\alpha}}{dT}(T, E_\nu) \phi_{\nu\alpha}(E_\nu) dE_\nu, \quad (3)$$

where N_e denotes the number of electrons in a detector and Δt is the exposure time and we assume $\Delta t = 10$ years for all the considered experiments. For ArCC, in which T is also the main observable, the event rate is computed in a similar way, except that N_e should be replaced by the number of argon nuclei. In our analysis, we also assume that the uncertainties on solar neutrino flux components [38] will improve and reach $\sim 1\%$ ⁴. The treatment of such uncertainties is incorporated by $\phi_{\text{total}} \rightarrow (1 + a)\phi_{\text{total}}$ where the normalization factor, a , is included with an uncertainty of $\sigma_a = 1\%$ and marginalized over in the χ^2 analysis.

For each channel and each experiment, we perform a binned χ^2 analysis to assess the sensitivity to the flux ratios (R_e, \bar{R}_μ) assuming the true value is $(0.3, 0.5)$. In Fig. 3, we show the results by considering several experiments individually as well as their combinations. The left panel shows how well the fluxes can be measured by using eES in HK (light blue) and ArCC in DUNE (light brown) as well as their combination (green). In the other two panels we add more experiments; the “pre.comb.” label in the legend of a given panel refers to the combination (green region) from the panel to the left. If all next-generation experiments are combined, and if the LS

experiments JUNO and THEIA can reach the optimal configurations of $T = 0.1$ MeV (denoted by subscript 1 in Fig. 3) we expect that \bar{R}_μ could be measured to the precision of 0.5 ± 0.15 . In such a case, the majority of neutrino events would arise from the interactions of solar pp neutrinos with $E_\nu \lesssim 0.4$ MeV.

Solar neutrinos as a probe of CP violation. In Fig. 4, we show $P_{\nu_e \rightarrow \nu_\alpha}(E_\nu)$ for various δ_{CP} values, obtained using the adiabatic approximation (for the range of its validity, see detailed discussion in [15]). As shown in the figure, $P_{\nu_e \rightarrow \nu_\mu}$ and $P_{\nu_e \rightarrow \nu_\tau}$ vary significantly for $\delta_{\text{CP}} \in [0, \pi]$; the variation can be as large as $\sim 50\%$. In making the figure, we have also included the matter effect for neutrinos propagating inside Earth; specifically, we have averaged over the day and the night values of $P_{\nu_e \rightarrow \nu_\alpha}$. Given the previous conclusion that the full flavor composition of solar neutrinos can be measured using NLO cross sections (see again Fig. 3), we expect that precision measurements of solar neutrinos should exhibit sensitivity to δ_{CP} . To demonstrate that, we performed a χ^2 analysis and the result is presented in Fig. 5. As shown in the figure, the full combination of next-generation detectors allows $\delta_{\text{CP}} = 0$ and $\delta_{\text{CP}} = \pi$ ($\pi/2$) to be differentiated at $\sim 1\sigma$ ($\sim 0.5\sigma$) CL. We also found that, for $\sigma_a \lesssim 0.1\%$, 2σ can be reached.

In making Fig. 5, we took δ_{CP} as the only fitting parameter and we fixed all other oscillation parameters at their present best fit values [39]. The reduction of uncertainties on the mixing angles, especially θ_{23} , is anticipated across relatively short time scales [40]. Currently, varying θ_{13} , θ_{12} , and θ_{23} within their 1σ ranges [39] would cause $P_{e\mu}$ to change by 0.2%, 2%, 4%, respectively. We leave a dedicated investigation on the correlation between the mixing angles and δ_{CP} to future work.

Summary and Conclusions. The survival probability of solar ν_e has been measured at a number of experiments in the ~ 1 –10 MeV energy range. On the other hand, directly measuring solar ν_μ and ν_τ fluxes is much more challenging and has not been performed to date.

³ In this work we are only concerned with the electron energy spectrum and we do not consider the angular spectrum which can be measured at HK and THEIA. Including the angular spectrum could in principle further improve the results.

⁴ We also implicitly assume that systematic uncertainties related to the detector are subleading. For instance, the present systematic uncertainties for Super-Kamiokande detector are already at $\mathcal{O}(1\%)$ level [31], and we anticipate further improvements for HK.

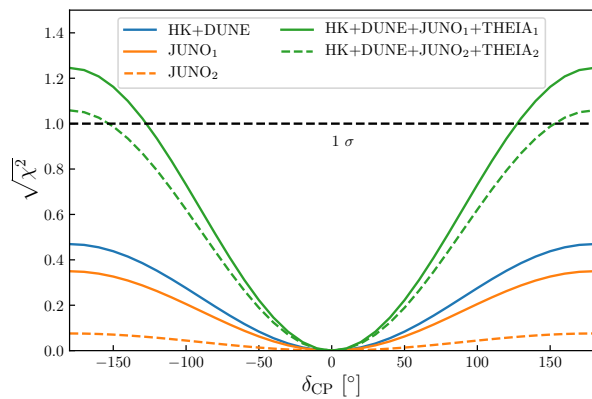


Figure 5. δ_{CP} sensitivity in solar neutrino measurements at next-generation neutrino experiments.

In this work, we propose a viable method to measure the flavor composition of solar neutrinos by utilizing differences between ν_μ and ν_τ eES cross sections. While these cross sections are identical at tree level, radiative corrections involving μ and τ leptons in loop diagrams induce an $\mathcal{O}(1\%)$ difference. This allows one to probe the flavor composition of solar neutrinos through the observation of electron recoil spectrum. We have quantified such an effect by studying the potential of several forthcoming neutrino detectors including HK, DUNE and JUNO, together with the proposed THEIA experiment. If THEIA and JUNO can realize 0.1 MeV detection threshold, then the $\mathcal{O}(1\%)$ difference in the cross sections would allow the combination of these experiments to effectively resolve the full flavor composition, see Fig. 3.

Furthermore, since $P_{\nu_e \rightarrow \nu_\mu}$ and $P_{\nu_e \rightarrow \nu_\tau}$ depend on δ_{CP} , the leptonic CP violation could be probed with solar neutrinos if the flavor-dependent radiative corrections are taken into consideration. We have assessed the sensitivity to δ_{CP} and found that $\sim 1\sigma$ CL can be reached in differentiating between $\delta_{\text{CP}} = 0$ and $\delta_{\text{CP}} = \pi$. This result would improve to $\sim 2\sigma$ provided that the uncertainties in solar neutrino flux reach sub-percent level. For such a measurement, the main experimental challenge would be low-threshold detection of solar neutrinos. Hence next-generation LS experiments like JUNO and THEIA will be particularly important.

Note Added. As we were finalizing this work, Ref. [41] appeared on arXiv. There, the authors scrutinize the prospects for measuring NLO effects with $\text{CE}\nu\text{NS}$ at next-generation dark matter experiments. While both $\text{CE}\nu\text{NS}$ and neutrino-electron scattering feature very small uncertainties in the cross section, the latter process has already been measured with large statistics while the coherent elastic neutrino-nucleus scattering is yet to be recorded for solar neutrinos. Hence, we regard neutrino-electron scattering channel as more promising for measuring the flavor composition of solar neutrinos at next-

generation experiments.

Acknowledgments. We would like to thank Leonardo Ferreira and Oleksandr Tomalak for very useful discussions. X.J.X is supported in part by the National Natural Science Foundation of China under grant No. 12141501 and also supported by CAS Project for Young Scientists in Basic Research (YSBR-099). X.J.X would also like to thank CERN for the hospitality and the financial support during his visit when this work was performed in part.

* vedran.brdar@cern.ch

† xuxj@ihep.ac.cn

- [1] R. Davis, Jr., D. S. Harmer, and K. C. Hoffman, *Search for neutrinos from the sun*, *Phys. Rev. Lett.* **20** (1968) 1205–1209.
- [2] J. N. Bahcall, N. A. Bahcall, and G. Shaviv, *Present status of the theoretical predictions for the Cl-36 solar neutrino experiment*, *Phys. Rev. Lett.* **20** (1968) 1209–1212.
- [3] B. Pontecorvo, *Neutrino Experiments and the Problem of Conservation of Leptonic Charge*, *Zh. Eksp. Teor. Fiz.* **53** (1967) 1717–1725.
- [4] V. N. Gribov and B. Pontecorvo, *Neutrino astronomy and lepton charge*, *Phys. Lett. B* **28** (1969) 493.
- [5] L. Wolfenstein, *Neutrino Oscillations in Matter*, *Phys. Rev. D* **17** (1978) 2369–2374.
- [6] S. P. Mikheyev and A. Yu. Smirnov, *Resonance Amplification of Oscillations in Matter and Spectroscopy of Solar Neutrinos*, *Sov. J. Nucl. Phys.* **42** (1985) 913–917. [*Yad. Fiz.*42,1441(1985)].
- [7] S. P. Mikheyev and A. Y. Smirnov, *Resonant amplification of neutrino oscillations in matter and solar neutrino spectroscopy*, *Nuovo Cim. C* **9** (1986) 17–26.
- [8] **SNO Collaboration**, Q. R. Ahmad *et al.*, *Measurement of the rate of $\nu_e + d \rightarrow p + p + e^-$ interactions produced by ^8B solar neutrinos at the Sudbury Neutrino Observatory*, *Phys. Rev. Lett.* **87** (2001) 071301, [[nucl-ex/0106015](#)].
- [9] **SNO Collaboration**, Q. R. Ahmad *et al.*, *Direct evidence for neutrino flavor transformation from neutral current interactions in the Sudbury Neutrino Observatory*, *Phys. Rev. Lett.* **89** (2002) 011301, [[nucl-ex/0204008](#)].
- [10] **Super-Kamiokande Collaboration**, S. Fukuda *et al.*, *Solar B-8 and hep neutrino measurements from 1258 days of Super-Kamiokande data*, *Phys. Rev. Lett.* **86** (2001) 5651–5655, [[hep-ex/0103032](#)].
- [11] **Super-Kamiokande Collaboration**, S. Fukuda *et al.*, *Determination of solar neutrino oscillation parameters using 1496 days of Super-Kamiokande I data*, *Phys. Lett. B* **539** (2002) 179–187, [[hep-ex/0205075](#)].
- [12] **Borexino Collaboration**, C. Arpesella *et al.*, *Direct Measurement of the Be-7 Solar Neutrino Flux with 192 Days of Borexino Data*, *Phys. Rev. Lett.* **101** (2008) 091302, [[0805.3843](#)].
- [13] **BOREXINO Collaboration**, M. Agostini *et al.*, *Experimental evidence of neutrinos produced in the*

- CNO fusion cycle in the Sun*, *Nature* **587** (2020) 577–582, [2006.15115].
- [14] M. Maltoni and A. Y. Smirnov, *Solar neutrinos and neutrino physics*, *Eur. Phys. J. A* **52** (2016), no. 4 87, [1507.05287].
- [15] X.-J. Xu, Z. Wang, and S. Chen, *Solar neutrino physics*, *Prog. Part. Nucl. Phys.* **131** (2023) 104043, [2209.14832].
- [16] **DUNE Collaboration**, R. Acciarri *et al.*, *Long-Baseline Neutrino Facility (LBNF) and Deep Underground Neutrino Experiment (DUNE): Conceptual Design Report, Volume 2: The Physics Program for DUNE at LBNF*, 1512.06148.
- [17] K. Abe *et al.*, *Letter of Intent: The Hyper-Kamiokande Experiment — Detector Design and Physics Potential* —, 1109.3262.
- [18] L. M. Sehgal, *Differences in the Coherent Interactions of ν_e , ν_μ and ν_τ* , *Phys. Lett. B* **162** (1985) 370–372.
- [19] G. Degrossi, A. Sirlin, and W. J. Marciano, *Effective Electromagnetic Form-factor of the Neutrino*, *Phys. Rev. D* **39** (1989) 287–294.
- [20] O. Tomalak, P. Machado, V. Pandey, and R. Plestid, *Flavor-dependent radiative corrections in coherent elastic neutrino-nucleus scattering*, *JHEP* **02** (2021) 097, [2011.05960].
- [21] S. Sarantakos, A. Sirlin, and W. J. Marciano, *Radiative Corrections to Neutrino-Lepton Scattering in the $SU(2)_L \times U(1)$ Theory*, *Nucl. Phys. B* **217** (1983) 84–116.
- [22] W. J. Marciano and Z. Parsa, *Neutrino electron scattering theory*, *J. Phys. G* **29** (2003) 2629–2645, [hep-ph/0403168].
- [23] O. Tomalak and R. J. Hill, *Theory of elastic neutrino-electron scattering*, *Phys. Rev. D* **101** (2020), no. 3 033006, [1907.03379].
- [24] R. J. Hill and O. Tomalak, *On the effective theory of neutrino-electron and neutrino-quark interactions*, *Phys. Lett. B* **805** (2020) 135466, [1911.01493].
- [25] **JUNO Collaboration**, F. An *et al.*, *Neutrino Physics with JUNO*, *J. Phys. G* **43** (2016), no. 3 030401, [1507.05613].
- [26] **THEIA Collaboration**, M. Askins *et al.*, *THEIA: an advanced optical neutrino detector*, *Eur. Phys. J. C* **80** (2020), no. 5 416, [1911.03501].
- [27] A. Sirlin and A. Ferroglia, *Radiative Corrections in Precision Electroweak Physics: a Historical Perspective*, *Rev. Mod. Phys.* **85** (2013), no. 1 263–297, [1210.5296].
- [28] F. J. Botella, C. S. Lim, and W. J. Marciano, *Radiative corrections to neutrino indices of refraction*, *Phys. Rev. D* **35** (Feb, 1987) 896–901.
- [29] H. Minakata and S. Watanabe, *Solar neutrinos and leptonic cp violation*, *Physics Letters B* **468** (1999), no. 3 256–260.
- [30] **SNO Collaboration**, B. Aharmim *et al.*, *Electron energy spectra, fluxes, and day-night asymmetries of $B-8$ solar neutrinos from measurements with NaCl dissolved in the heavy-water detector at the Sudbury Neutrino Observatory*, *Phys. Rev. C* **72** (2005) 055502, [nucl-ex/0502021].
- [31] **Super-Kamiokande Collaboration**, K. Abe *et al.*, *Solar Neutrino Measurements in Super-Kamiokande-IV*, *Phys. Rev. D* **94** (2016), no. 5 052010, [1606.07538].
- [32] J. F. Beacom, W. M. Farr, and P. Vogel, *Detection of supernova neutrinos by neutrino proton elastic scattering*, *Phys. Rev. D* **66** (2002) 033001, [hep-ph/0205220].
- [33] **Borexino Collaboration**, M. Agostini *et al.*, *Identification of the cosmogenic ^{11}C background in large volumes of liquid scintillators with Borexino*, *Eur. Phys. J. C* **81** (2021), no. 12 1075, [2106.10973].
- [34] **Borexino Collaboration**, G. Bellini *et al.*, *Final results of Borexino Phase-I on low energy solar neutrino spectroscopy*, *Phys. Rev. D* **89** (2014), no. 11 112007, [1308.0443].
- [35] F. Capozzi, S. W. Li, G. Zhu, and J. F. Beacom, *DUNE as the Next-Generation Solar Neutrino Experiment*, *Phys. Rev. Lett.* **123** (2019), no. 13 131803, [1808.08232].
- [36] https://indico.cern.ch/event/466934/contributions/2580153/attachments/1488652/2313013/EPS_HEP_nrossi.pdf.
- [37] G. Bellini, *The impact of Borexino on the solar and neutrino physics*, *Nucl. Phys. B* **908** (2016) 178–198.
- [38] J. Bergstrom, M. C. Gonzalez-Garcia, M. Maltoni, C. Pena-Garay, A. M. Serenelli, and N. Song, *Updated determination of the solar neutrino fluxes from solar neutrino data*, *JHEP* **03** (2016) 132, [1601.00972].
- [39] I. Esteban, M. C. Gonzalez-Garcia, M. Maltoni, T. Schwetz, and A. Zhou, *The fate of hints: updated global analysis of three-flavor neutrino oscillations*, *JHEP* **09** (2020) 178, [2007.14792].
- [40] N. Song, S. W. Li, C. A. Argüelles, M. Bustamante, and A. C. Vincent, *The Future of High-Energy Astrophysical Neutrino Flavor Measurements*, *JCAP* **04** (2021) 054, [2012.12893].
- [41] N. Mishra and L. E. Strigari, *Solar neutrinos with CEvNS and flavor-dependent radiative corrections*, 2305.17827.